

Performance Analysis of Dense SCNs with Generalized Shadowing/Fading and NLOS/LOS Transmissions

Bin Yang, *Student Member, IEEE*, Guoqiang Mao, *Senior Member, IEEE*, Ming Ding,
Member, IEEE, Xiaohu Ge, *Senior Member, IEEE*, Xiaofeng Tao, *Senior Member, IEEE*

Abstract

In this paper, we propose a unified framework to analyze the performance of dense small cell networks (SCNs) in terms of the coverage probability and the area spectral efficiency (ASE). A practical path loss model incorporating both non-line-of-sight (NLOS) and line-of-sight (LOS) transmissions has been considered in our analysis. Moreover, we adopt a generalized shadowing/fading model, in which log-normal shadowing and/or Rayleigh fading can be treated in a unified framework. The coverage probability and the ASE are derived, using a generalized stochastic geometry analysis based on a transformed Poisson point process (PPP). Using the analysis, we show for the first time that depending on the intensity of the BSs, the performance of the SCNs can be divided into four different regimes, i.e., the noise-limited regime, the signal NLOS-to-LOS-transition regime, the interference NLOS-to-LOS-transition regime and the dense interference-limited regime, where

Correspondence author: Prof. Xiaohu Ge (Email: xhge@mail.hust.edu.cn, Tel: +86-27-87557941 ext 822).

Bin Yang and Xiaohu Ge are with the School of Electronic Information and Communications, Huazhong University of Science and Technology, China (Email: yangbin@hust.edu.cn, xhge@mail.hust.edu.cn). Bin Yang would like to acknowledge the support from the China Scholarship Council (CSC). Xiaohu Ge's research is supported by the National Natural Science Foundation of China (NSFC) (Grant No. 61210002), the Fundamental Research Funds for the Central Universities (Grant No. 2015XJGH011), and China International Joint Research Center of Green Communications and Networking (No. 2015B01008).

Guoqiang Mao is with the School of Computing and Communication, The University of Technology Sydney, Australia. He also holds adjunct positions at Data61, CSIRO, Australia, the School of Electronic Information & Communications, Huazhong University of Science & Technology, Wuhan, China, and the School of Information and Communication Engineering, Beijing University of Posts and Telecommunications, Beijing, China (e-mail: g.mao@ieee.org). Guoqiang Mao's research is supported by Australian Research Council (ARC) Discovery project DP110100538 and Chinese National Science Foundation project 61428102.

Ming Ding is with Data61, CSIRO, Australia (Email: ming.ding@data61.csiro.au).

Xiaofeng Tao is with the National Engineering Lab. for Mobile Network Security, Beijing University of Posts and Telecommunications, China. (Email: taoxf@bupt.edu.cn).

in each regime the performance is dominated by different factors. The analysis helps to understand as the intensity of the BSs grows continually, which dominant factor that determines the cellular network performance and therefore provide guidance on the design and management of the cellular networks as we evolve into dense SCNs.

Index Terms

Stochastic geometry, dense small cellular networks, non-line-of-sight (NLOS), line-of-sight (LOS), cell association, generalized shadowing/fading, log-normal shadowing, Rayleigh fading, Poisson point process (PPP), coverage probability, area spectral efficiency (ASE).

I. INTRODUCTION

With skyrocketing demands on wireless data driven by smartphones, tablets, and video streaming, data traffic is expected to overwhelm cellular networks in the near future. The annual visual network index (VNI) reports released by Cisco revealed that an incremental approach will not come close to meeting the demands that networks will face by 2020 [1, 2]. Against this background, network densification, together with millimeter wave technology and massive multiple-input multiple-output technology, have been envisioned to be “the three pillars” to support the vision of the emerging fifth generation (5G) wireless networks in the future [3]. In this context, the orthogonal deployment of dense small cellular networks (SCNs) [4, 5] has been selected as the workhorse for capacity enhancement in the fourth generation (4G) and the 5G networks developed by the third Generation Partnership Project (3GPP). In this paper, we focus on the performance analysis of these dense SCNs.

Different from most previous work where the propagation path loss between the base stations (BSs) and the mobile users (MUs) is assumed to follow the same power-law model, irrespective of their distance, in this paper we consider both non-line-of-sight (NLOS) and line-of-sight (LOS) transmissions, which frequently occur in *urban areas*. More specifically, BSs deployed according to a homogeneous Poisson point process (PPP) are divided into two categories, i.e., NLOS BSs and LOS BSs, depending on the distance between the BSs and the interested MU. In this context, the authors of [6] studied the coverage and capacity performance by using a multi-slop path loss model incorporating probabilistic NLOS and LOS transmissions. Millimeter wave cellular networks with NLOS and LOS transmissions

were investigated in [7–10]. Kamel *et al.* proposed a multiple association scheme as a solution to distribute the traffic load of the MU to multiple small cells in the MU’s neighborhood in dense SCNs [11]. In this work, we will study the performance impact of NLOS-to-LOS transition in dense SCNs in urban areas with a generalized shadowing/fading model. The main contributions of this paper are as follows:

- A general SCN model: For characterizing the signal-to-interference-plus-noise ratio (SINR) coverage probability and the ASE in SCNs, a unified framework is proposed in Section V, which is applicable to analyze a SCN using the strongest received signal power association, assuming generalized shadowing/fading and incorporating both NLOS and LOS transmissions.
- Theoretical analysis: In Section VII, the coverage probability and the ASE are derived based on the proposed model incorporating LOS/NLOS transmissions and/or shadow fading. The accuracy of our analytical results is validated by Monte Carlo simulations.
- Performance insights: Different from existing work that does not differentiate NLOS and LOS transmissions and that does not consider shadow fading, our analysis demonstrates that incorporating both NLOS and LOS transmissions into the path loss model has a significant impact on network performance. More specifically, our analysis shows for the first time that depending on the intensity of the BSs, the performance of the SCNs can be divided into four different regimes where in each regime the performance is dominated by different factors. The analysis helps to understand as the intensity of the BSs grows continually, which dominant factor that determines the cellular network performance and therefore provide guidance on the design and management of the cellular networks as we evolve into dense SCNs.

The remainder of this paper is organized as follows. In Section II, motivations and some recent work closely related to ours are presented. Section III introduces the system model and network assumptions. An important theorem used in the analysis on transforming the original network into an equivalent distance-dependent network, i.e., the Equivalence Theorem, is presented and proven in Section IV, followed by an application of the theorem to derive the distribution of the strongest received signal power. Section V studies the coverage probability

and the ASE of the SCNs. In Section VI, a comparison with other cell association scheme is provided. In Section VII, the analytical results are validated via Monte Carlo simulations and the performances of the SCNs in different scenarios are elaborated. Finally, Section VIII concludes this paper and discusses possible future work.

II. MOTIVATIONS AND RELATED WORK

The modeling of the spatial distribution of small cells using stochastic geometry has resulted in significant progress in understanding the performance of cellular networks [12, 13]. Random spatial point processes, especially the homogeneous PPP, have now been widely used to model the locations of small cell BSs in various scenarios. However, the existing results are usually based on certain simplified assumptions, e.g., Rayleigh fading, a single path loss exponent with no thermal noise, etc, for analytical tractability, which may not hold in a more realistic scenario. For instance, consider a SCN in urban areas, the path loss model may not follow a single power law relationship in the near field and hence non-singular or multiple-slope path loss model [14] should be applied. Besides, signal transmissions between BSs and MUs are frequently affected by reflection, diffraction, and even blockage due to high-rise buildings in urban areas, and thus NLOS/LOS transmissions should also be considered [7]. As a consequence, a more generalized propagation model incorporating both NLOS and LOS transmissions is needed to cope with these new characteristics especially for dense SCNs in urban areas.

A number of more recent work had a new look at dense SCNs considering more practical propagation models. The closest related work to the one in this paper are in [6–9, 15]. In [6] and [7], the coverage probability and capacity were calculated based on the smallest path loss cell association model assuming multi-path fading modeled as Rayleigh fading and Nakagami- m fading, respectively. However, shadowing was ignored in their models, which may not be very practical for a SCN. The authors of [8] and [9] analyzed the coverage and capacity performance in millimeter wave cellular networks. In [8], a three-state statistical model for each link was assumed, in which a link can either be in a NLOS, LOS or in an outage state. In [9], self-backhauled millimeter wave cellular networks were analyzed assuming a cell association scheme based on the smallest path loss. Besides, both [8] and

[9] assumed a noise-limited network ignoring inter-cell interference, which may not be very practical since modern wireless networks generally work in an interference-limited region. In [15], the authors assumed Rayleigh fading for NLOS transmissions and Nakagami- m fading for LOS transmissions which is more practical than work in [6]. However, the cell association scheme in [15] is only applicable to the scenario where the SINR threshold is greater than 0 dB. Besides, the ASE performance was not analyzed in [15].

To summarize, in this paper, we propose a more generalized framework for the performance analysis of dense SCNs in urban areas compared with the work in [6–9, 15]. Our framework takes into account a cell association scheme based on the strongest received signal power, probabilistic NLOS and LOS transmissions, multi-path fading and/or shadowing. Furthermore, the proposed framework can also be applied to analyze dense SCNs, where BSs are distributed according to non-homogeneous PPPs, i.e., the BS intensity is spatially varying.

III. SYSTEM MODEL

We consider a homogeneous SCN in urban areas and focus on the analysis of downlink performance. Assume that BSs are spatially distributed on an infinite plane and the locations of BSs \mathbf{X}_i follow an independent PPP denoted by $\Phi = \{\mathbf{X}_i\}$ with an intensity of λ , where i is the BS index. MUs are deployed according to another independent homogeneous PPP denoted by Φ_u with an intensity of λ_u . All BSs in the network operate at the same power P_t and share the same bandwidth. Within a cell, MUs use orthogonal frequencies for downlink transmissions and therefore *intra-cell interference* is not considered in our analysis. However, adjacent BSs may generate *inter-cell interference* to MUs, which is the main focus of our work.

A. Path Loss Model

We incorporate both NLOS and LOS transmissions into the path loss model, whose performance impact is attracting growing interest among researchers recently. In reality, the occurrence of NLOS or LOS transmissions depends on various environmental factors, including geographical structure, distance and clusters, etc. The following definition gives a simplified one-parameter model of NLOS and LOS transmissions.

Definition 1. The occurrence of NLOS and LOS transmissions can be modeled using probabilities $p^{\text{NL}}(R_i)$ and $p^{\text{L}}(R_i)$, respectively. The probabilities are functions of the distance between a BS and a MU which satisfy

$$p^{\text{NL}}(R_i) + p^{\text{L}}(R_i) = 1, \quad (1)$$

where $R_i = \|\mathbf{X}_i\|$ denotes the Euclidean distance between a BS at \mathbf{X}_i and the typical MU (alternatively called the probe MU or the tagged MU) located at the origin o .

Regarding the mathematical form of $p^{\text{L}}(R_i)$ (or $p^{\text{NL}}(R_i)$), N. Blaunstein [16] formulated $p^{\text{L}}(R_i)$ as a negative exponential function, i.e., $p^{\text{L}}(R_i) = e^{-\kappa R_i}$, where κ is a parameter determined by the intensity and the mean length of the blockages lying in the visual path between the typical MU and BSs. Bai [17] extended N. Blaunstein's work by using random shape theory which shows that κ is not only determined by the mean length but also the mean width of the blockages. The authors of [8] and [17] approximated $p^{\text{L}}(R_i)$ by using piecewise functions and step functions, respectively. The authors of [6] considered $p^{\text{L}}(R_i)$ to be a linear function and a two-piece exponential function, respectively; both are recommended by the 3GPP.

It should be noted that the occurrence of NLOS (or LOS) transmissions is assumed to be independent for different BS-MU pairs. Though such assumption might not be entirely realistic (e.g., NLOS transmissions caused by a large obstacle may be spatially correlated), the authors of [17] showed that the impact of the independence assumption on the SINR analysis is negligible.

Note that from the viewpoint of the typical MU, each BS in the infinite plane \mathbb{R}^2 is either a NLOS BS or a LOS BS to the typical MU. Accordingly, we perform a thinning procedure on points in the PPP Φ to model the distributions of NLOS BSs and LOS BSs, respectively. That is, each BS in Φ will be kept if a BS has a NLOS transmission with the typical MU, thus forming a new point process denoted by Φ^{NL} . While BSs in $\Phi \setminus \Phi^{\text{NL}}$ form another point process denoted by Φ^{L} , representing the set of BSs with LOS path to the typical MU. As a consequence of the independence assumption of LOS and NLOS transmissions mentioned in the last paragraph, Φ^{NL} and Φ^{L} are two independent non-homogeneous PPPs with intensity

functions $\lambda p^{\text{NL}}(R_i)$ and $\lambda p^{\text{L}}(R_i)$, respectively.

In general, NLOS and LOS transmissions incur different path losses, which are captured by the following equations¹

$$PL_{\text{dB}}^{\text{NL}} = A_{\text{dB}}^{\text{NL}} + \alpha^{\text{NL}} 10 \log_{10} R + \xi_{\text{dB}}^{\text{NL}}, \quad (2)$$

and

$$PL_{\text{dB}}^{\text{L}} = A_{\text{dB}}^{\text{L}} + \alpha^{\text{L}} 10 \log_{10} R + \xi_{\text{dB}}^{\text{L}}, \quad (3)$$

where the path loss is expressed in dB unit, $A_{\text{dB}}^{\text{NL}}$ and A_{dB}^{L} are the path losses at the reference distance (usually at 1 meter), α^{NL} and α^{L} are respective path loss exponents for NLOS and LOS transmissions, $\xi_{\text{dB}}^{\text{NL}}$ and $\xi_{\text{dB}}^{\text{L}}$ are independent Gaussian random variables with zero means, i.e., $\xi_{\text{dB}}^{\text{NL}} \sim \mathcal{N}(0, (\sigma^{\text{NL}})^2)$ and $\xi_{\text{dB}}^{\text{L}} \sim \mathcal{N}(0, (\sigma^{\text{L}})^2)$, reflecting the signal attenuation caused by shadow fading. The corresponding model parameters can be found in [18–22].

Accordingly, the received signal power for NLOS and LOS transmissions in W (watt) can be expressed by

$$P_i^{\text{NL}} = B^{\text{NL}} \mathcal{H}^{\text{NL}}(R_i)^{-\alpha^{\text{NL}}} \quad (4)$$

and

$$P_i^{\text{L}} = B^{\text{L}} \mathcal{H}^{\text{L}}(R_i)^{-\alpha^{\text{L}}}, \quad (5)$$

respectively, where $\mathcal{H}^{\text{NL}} = \exp(\beta \xi_{\text{dB}}^{\text{NL}})$ (or $\mathcal{H}^{\text{L}} = \exp(\beta \xi_{\text{dB}}^{\text{L}})$) denotes log-normal shadowing for NLOS (or LOS) transmission, $R_i = \|\mathbf{X}_i\|$ denotes the distance between the typical MU located at the origin o and the BS at X_i , and $B^{\text{NL}} = P_t \cdot 10^{-A_{\text{dB}}^{\text{NL}}/10}$, $B^{\text{L}} = P_t \cdot 10^{-A_{\text{dB}}^{\text{L}}/10}$ and $\beta = -\ln 10/10$ are constants.

Therefore, the received power by the typical MU from BS \mathbf{X}_i is given by

$$P_i(R_i) = \mathbb{I}_i P_i^{\text{NL}} + (1 - \mathbb{I}_i) P_i^{\text{L}}, \quad (6)$$

where \mathbb{I}_i is a random indicator variable, which equals to 1 for NLOS transmission and 0 for

¹As the derivations in scenarios with log-normal shadowing is much more complicated than that with Rayleigh fading, we choose to take the former as an example. It is found in Eq. (4) and Eq. (5) that the model can also be applied to Rayleigh fading and other generalized shadowing/fading models.

LOS transmission, and the corresponding probabilities are $p^{\text{NL}}(R_i)$ and $p^{\text{L}}(R_i)$, respectively, i.e.,

$$\mathbb{I}_i = \begin{cases} 1, & \text{with probability } p^{\text{NL}}(R_i) \\ 0, & \text{with probability } p^{\text{L}}(R_i) \end{cases}. \quad (7)$$

Based on the path loss model discussed above, for downlink transmissions, the SINR experienced by the typical MU associated with BS \mathbf{X}_i can be written by

$$\text{SINR}_i = \frac{S}{I + \eta} = \frac{P_i(R_i)}{\sum_{\mathbf{X}_z \in \Omega'} P_z(R_z) + \eta}, \quad (8)$$

where Ω' is the Palm point process [23] representing the set of interfering BSs in the network to the typical MU and η denotes the noise at the MU side, which is assumed to be additive white Gaussian noise (AWGN).

B. Cell Association Scheme

Considering NLOS and LOS transmissions, the typical MU should connect with the BS that provides the highest SINR. Such BS does not necessarily have to be the nearest BS from the typical MU in the SCN. More specifically, the typical MU associates itself to the BS \mathbf{X}_i^* given by

$$\mathbf{X}_i^* = \arg \max_{\mathbf{X}_i \in \Phi} \text{SINR}_i. \quad (9)$$

Intuitively, the highest SINR association is equivalent to the strongest received signal power association. Such intuition is formally presented and proved in Lemma 2.

Lemma 2. For a non-negative set $\Xi = \{a_q\}$, $q \in \mathbb{N}$, $\frac{a_m}{\sum_{q \neq m} a_q + W} > \frac{a_n}{\sum_{q \neq n} a_q + W}$ if and only if $a_m > a_n$, $\forall a_m, a_n \in \Xi$.

Proof: For a non-negative set $\Xi = \{a_q\}$, $q \in \mathbb{N}$, $\frac{a_m}{\sum_q a_q + W} > \frac{a_n}{\sum_q a_q + W}$ if and only if $a_m > a_n$, thus $\frac{a_m}{\sum_q a_q + W - a_m} > \frac{a_n}{\sum_q a_q + W - a_n}$ if and only if $a_m > a_n$, which completes the proof. ■

Lemma 2 states that providing the highest SINR is equivalent to providing the strongest received power to the typical MU. It follows from Eq. (9) and Lemma 2 that the BS associated

with the typical MU can also be written as

$$(\mathbf{X}_i, \mathbf{U})^* = \arg \max_{(\mathbf{X}_i, \mathbf{U}) \in \mathbb{S}} B^{\mathbf{U}} \mathcal{H}^{\mathbf{U}} (R_i)^{-\alpha^{\mathbf{U}}}, \quad (10)$$

where $\mathbf{X}_i \in \Phi$, $\mathbf{U} \in \{\text{NL}, \text{L}\}$ and the set $\mathbb{S} = \Phi \times \{\text{NL}, \text{L}\}$. In the following, we mainly use Eq. (10) to characterize the considered cell association scheme.

IV. THE EQUIVALENCE OF SCNs AND THE DISTRIBUTION OF THE STRONGEST RECEIVED SIGNAL POWER

Before presenting our main analytical results, first we introduce the Equivalence Theorem that will be used throughout the paper. The purpose of introducing the Equivalence Theorem is to unify the analysis considering different multi-path fading and/or shadowing, and to reduce the complexity of our theoretical analysis. Then based on this theorem, we derive the cumulative distribution function (CDF) of the strongest received signal power.

A. The Equivalence of SCNs

In this subsection, an equivalent SCN to the one being analyzed will be introduced, which specifies how the intensity measure and the intensity are changed after a transformation of original PPPs. More specifically, denoting by

$$\overline{R}_i^{\text{NL}} = R_i \cdot (B^{\text{NL}} \mathcal{H}^{\text{NL}})^{-1/\alpha^{\text{NL}}} \quad (11)$$

and

$$\overline{R}_i^{\text{L}} = R_i \cdot (B^{\text{L}} \mathcal{H}^{\text{L}})^{-1/\alpha^{\text{L}}}, \quad (12)$$

the received signal power in Eq. (4) and Eq. (5) can be written as

$$P_i^{\text{NL}} = \left(\overline{R}_i^{\text{NL}} \right)^{-\alpha^{\text{NL}}} \quad (13)$$

and

$$P_i^{\text{L}} = \left(\overline{R}_i^{\text{L}} \right)^{-\alpha^{\text{L}}}. \quad (14)$$

From the discussion in Subsection III-A, the BS's location $\{\mathbf{X}_i\}_{i \in \mathbb{N}}$ can be viewed as a non-homogeneous PPP with an equivalent intensity of $\lambda p^{\text{NL}}(R_i)$. Through the above transformation which scales the distances between the typical MU and all other BSs using Eq. (11) and (12), the scaled point process for NLOS BSs (or LOS BSs) still remains a PPP denoted by $\overline{\Phi}^{\text{NL}}$ (or $\overline{\Phi}^{\text{L}}$) according to the displacement theorem [24]. The intuition is that in the equivalent networks, the received signal power and cell association scheme are only dependent on the new equivalent distance $\overline{R}_i^{\text{NL}}$ (or $\overline{R}_i^{\text{L}}$) between the BSs and the typical MU, while the effects of transmit power, multi-path fading and shadowing are incorporated into the equivalent intensity (or the equivalent intensity measure) of the transformed point process. Besides, $\overline{\Phi}^{\text{NL}}$ and $\overline{\Phi}^{\text{L}}$ are mutually independent because of the independence between Φ^{NL} and Φ^{L} . As a result, the performance analysis involving path loss, multi-path fading, shadowing, etc, can be handled in a unified framework. This motivates the following theorem.

Theorem 3 (The Equivalence Theorem). *Assume that a general fading or shadowing satisfy $\mathbb{E}_{\mathcal{H}^U} \left[(\mathcal{H}^U)^{2/\alpha^U} \right] < \infty$. The system which consists of two non-homogeneous PPPs with intensities $\lambda p^{\text{NL}}(R_i)$ and $\lambda p^{\text{L}}(R_i)$ respectively, representing the sets of NLOS and LOS BSs, and in which each MU is associated with the BS providing the strongest received signal power is equivalent, in terms of performance to the typical MU located at the origin, to another system consisting of two non-homogeneous PPPs with intensities $\lambda^{\text{NL}}(\cdot)$ and $\lambda^{\text{L}}(\cdot)$ respectively, representing the sets of NLOS and LOS BSs, and in which the typical MU is associated with the nearest BS. Moreover, intensities $\lambda^{\text{NL}}(\cdot)$ and $\lambda^{\text{L}}(\cdot)$ are given by*

$$\lambda^{\text{NL}}(t) = \frac{d}{dt} \Lambda^{\text{NL}}([0, t]) \quad (15)$$

and

$$\lambda^{\text{L}}(t) = \frac{d}{dt} \Lambda^{\text{L}}([0, t]), \quad (16)$$

respectively, where

$$\Lambda^{\text{NL}}([0, t]) = \mathbb{E}_{\mathcal{H}^{\text{NL}}} \left[2\pi \lambda \int_{R_i=0}^{t(B^{\text{NL}} \mathcal{H}^{\text{NL}})^{1/\alpha^{\text{NL}}}} p^{\text{NL}}(R_i) R_i dR_i \right] \quad (17)$$

and

$$\Lambda^L([0, t]) = \mathbb{E}_{\mathcal{H}^L} \left[2\pi\lambda \int_{R_i=0}^{t(B^L \mathcal{H}^L)^{1/\alpha^L}} p^L(R_i) R_i dR_i \right]. \quad (18)$$

Proof: See Appendix A. ■

By utilizing the Equivalence theorem above, the transformed cellular network has the exactly same performance for the typical MU with respect to the coverage probability and the ASE compared with the original network, which is proved in Appendix A and validated by Monte Carlo simulations in Section VII. After transformation, the received signal power and cell association scheme are only dependent on the equivalent distance between the BSs and the typical MU, i.e., $\overline{R_i^{NL}}$ and $\overline{R_i^L}$, while the effects of transmit power, multi-path fading and shadowing are incorporated into the equivalent intensity shown in Eq. (15) and Eq. (16). Therefore, the complexity of performance analysis can be significantly reduced.

Remark 4. From Lemma 2 and Theorem 3, any cell association scheme without considering the status of BSs and MUs, e.g., traffic load, spectrum usage of BSs and the battery capacity of MUs, is equivalent to or can be transformed to the nearest BS cell association scheme.

Remark 5. In our system model, log-normal shadowing is assumed. Thus the condition of $\mathbb{E}_{\mathcal{H}^U} \left[(\mathcal{H}^U)^{2/\alpha^U} \right] < \infty$ is satisfied. For a general case of shadowing and/or fading model, $\mathbb{E}_{\mathcal{H}^U} \left[(\mathcal{H}^U)^{2/\alpha^U} \right] < \infty$ can be easily met due to the bounded fading in practice.

In the next subsection, we will provide an application of the Equivalence theorem, i.e., using the equivalence theorem to derive the distribution of the strongest received signal power.

B. The Distribution of the Strongest Received Signal Power

In this subsection, we use stochastic geometry and Theorem 3 to obtain the distribution of the strongest received signal power. Then we will use simulation results to validate our theoretical analysis.

Lemma 6. Denote the strongest received signal power as \mathcal{P} , i.e., $\mathcal{P} = \max(P_i)$, the distribution of the strongest received signal power by the typical MU can be given by

$$\Pr[\mathcal{P} \leq \gamma] = \exp \left[-\Lambda^{NL} \left(\left[0, \gamma^{-1/\alpha^{NL}} \right] \right) - \Lambda^L \left(\left[0, \gamma^{-1/\alpha^L} \right] \right) \right], \quad (19)$$

where $\Lambda^{\text{NL}}([0, t])$ and $\Lambda^{\text{L}}([0, t])$ are defined in Eq. (17) and Eq. (18), respectively.

Proof: See Appendix B. ■

If a specific NLOS/LOS transmission model is given, the distribution of the strongest received signal power can be easily derived using Lemma 6. The following is an example assuming that the LOS transmission probability follows a negative exponential distribution.

Assume that $p^{\text{L}}(R_i) = e^{-\kappa R_i}$ and $p^{\text{NL}}(R_i) = 1 - e^{-\kappa R_i}$, where κ is a constant determined by the density and the mean length of blockages lying in the visual path between the typical MU and the connected BS [7], then the CDF of the strongest received signal power is given by

$$\Pr[\mathcal{P} \leq \gamma] = \exp \left[-\Lambda^{\text{NL}} \left(\left[0, \gamma^{-1/\alpha^{\text{NL}}} \right] \right) - \Lambda^{\text{L}} \left(\left[0, \gamma^{-1/\alpha^{\text{L}}} \right] \right) \right], \quad (20)$$

where

$$\begin{aligned} \Lambda^{\text{NL}}([0, t]) &= \mathbb{E}_{\mathcal{H}^{\text{NL}}} \left\{ 2\pi\lambda \int_{R_i=0}^{t(B^{\text{NL}}\mathcal{H}^{\text{NL}})^{1/\alpha^{\text{NL}}}} p^{\text{NL}}(R_i) R_i dR_i \right\} \\ &= \int_{\mathcal{H}^{\text{NL}}=0}^{\infty} \frac{\mathcal{A} e^{-(\ln \mathcal{H}^{\text{NL}})^2/2(\sigma^{\text{NL}})^2}}{\mathcal{H}^{\text{NL}} \sigma^{\text{NL}} \sqrt{2\pi}} d\mathcal{H}^{\text{NL}}, \end{aligned} \quad (21)$$

where

$$\begin{aligned} \mathcal{A} &= \frac{\pi\lambda}{\kappa^2} \left[2 \left(\kappa t (B^{\text{NL}}\mathcal{H}^{\text{NL}})^{1/\alpha^{\text{NL}}} \right) e^{-\kappa t (B^{\text{NL}}\mathcal{H}^{\text{NL}})^{1/\alpha^{\text{NL}}}} \right. \\ &\quad \left. + \left(\kappa t (B^{\text{NL}}\mathcal{H}^{\text{NL}})^{1/\alpha^{\text{NL}}} \right)^2 - 2 \right]. \end{aligned} \quad (22)$$

And

$$\Lambda^{\text{L}}([0, t]) = \int_{\mathcal{H}^{\text{L}}=0}^{\infty} \frac{\mathcal{B} e^{-(\ln \mathcal{H}^{\text{L}})^2/2(\sigma^{\text{L}})^2}}{\mathcal{H}^{\text{L}} \sigma^{\text{L}} \sqrt{2\pi}} d\mathcal{H}^{\text{L}}, \quad (23)$$

where

$$\mathcal{B} = \frac{\pi\lambda}{\kappa^2} \left[1 - \left(\kappa t (B^{\text{L}}\mathcal{H}^{\text{L}})^{1/\alpha^{\text{L}}} + 1 \right) e^{-\kappa t (B^{\text{L}}\mathcal{H}^{\text{L}})^{1/\alpha^{\text{L}}}} \right]. \quad (24)$$

Fig. 1 illustrates the CDF of the strongest received signal power based on Eq. (20) and it can be seen that the simulation results perfectly match the analytical results. From Fig. 1, we can find that over 50% of the strongest received signal power is larger than -51 dBm when $\lambda = 10$ BSs/km² and this value increases by approximately 16 dB when $\lambda = 100$ BSs/km², which

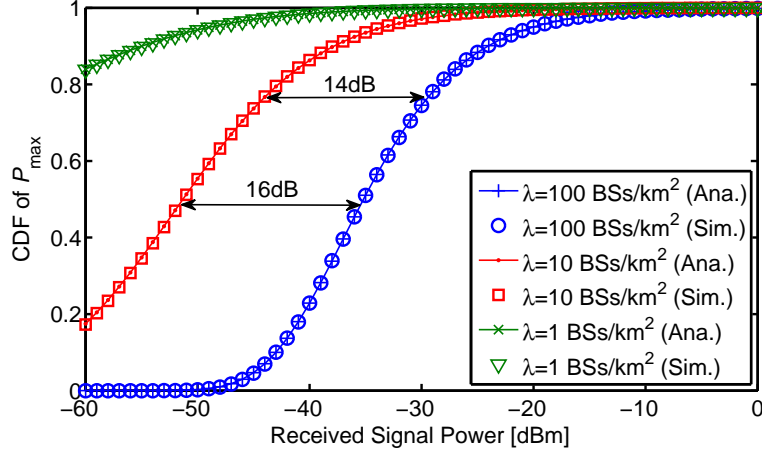


Figure 1. CDF of the strongest received signal power (simulation and analytical results), $P_t = 1$ W (30 dBm), log-normal shadowing with zero means, $\sigma^{\text{NL}} = 4$ dB and $\sigma^{\text{L}} = 3$ dB.

indicates that the strongest received signal power improves as the BS intensity increases.

V. THE COVERAGE PROBABILITY AND ASE ANALYSIS

In downlink performance evaluation, for networks where BSs are random distributed according to a PPP, it is sufficient to study the performance of the typical MU located at the origin o to characterize the performance of the SCN using the Palm theory [23, Eq. (4.71)]. In this section, the coverage probability is firstly investigated and then the ASE will be derived from the results of coverage probability.

The coverage probability is generally defined as the probability that the typical MU's measured SINR is greater than a designated threshold T , i.e.,

$$p_c(\lambda, T) = \Pr[\text{SINR} > T], \quad (25)$$

where the definition of SINR is given by Eq. (8) and the subscript i is omitted here for simplicity. Now, we present a main result in this section on the coverage probability as follows.

Theorem 7 (Coverage Probability). *Given that the signal propagation model follows Eq. (6) and the typical MU selects the serving BS according to Eq. (10), then the coverage probability*

$p_c(\lambda, T)$ can be evaluated by

$$p_c(\lambda, T) = p_c^L(\lambda, T) + p_c^{NL}(\lambda, T), \quad (26)$$

where

$$\begin{aligned} p_c^L(\lambda, T) = & \int_{y=0}^{\infty} \int_{\omega=-\infty}^{\infty} \left[\frac{1 - e^{-j\omega/T}}{2\pi j\omega} \right] \lambda^L(y) \exp\left\{ -\Lambda^{NL}\left([0, y^{\alpha^L/\alpha^{NL}}]\right) \right. \\ & - \Lambda^L([0, y]) + j\omega\eta y^{\alpha^L} + \int_{t=y^{\alpha^L/\alpha^{NL}}}^{\infty} \left[e^{j\omega y^{\alpha^L} t^{-\alpha^{NL}}} - 1 \right] \lambda^{NL}(t) dt \\ & \left. + \int_{t=y}^{\infty} \left[e^{j\omega(y/t)^{\alpha^L}} - 1 \right] \lambda^L(t) dt \right\} d\omega dy \end{aligned} \quad (27)$$

and

$$\begin{aligned} p_c^{NL}(\lambda, T) = & \int_{y=0}^{\infty} \int_{\omega=-\infty}^{\infty} \left[\frac{1 - e^{-j\omega/T}}{2\pi j\omega} \right] \lambda^{NL}(y) \exp\left\{ -\Lambda^L\left([0, y^{\alpha^{NL}/\alpha^L}]\right) \right. \\ & - \Lambda^{NL}([0, y]) + j\omega\eta y^{\alpha^{NL}} + \int_{t=y^{\alpha^{NL}/\alpha^L}}^{\infty} \left[e^{j\omega y^{\alpha^{NL}} t^{-\alpha^L}} - 1 \right] \lambda^L(t) dt \\ & \left. + \int_{t=y}^{\infty} \left[e^{j\omega(y/t)^{\alpha^{NL}}} - 1 \right] \lambda^{NL}(t) dt \right\} d\omega dy, \end{aligned} \quad (28)$$

where $j = \sqrt{-1}$ denotes the imaginary unit, $\lambda^{NL}(\cdot)$ and $\lambda^L(\cdot)$ are defined in Theorem 3.

Proof: See Appendix C. ■

The coverage probability evaluated by Eq. (26) in Theorem 7 is at least a 3-fold integral which is complicated for numerical computation. However, Theorem 7 gives general results that can be applied to various multi-path fading or shadowing models, e.g., Rayleigh fading, Nakagami- m fading, etc, and various NLOS/LOS transmission models as well.

In the following, we focus on studying a special scenario in which only log-normal shadowing is considered and fast fading is ignored. Besides, a simplified NLOS/LOS transmission model is adopted for ease of numerical evaluations, which is expressed as follows

$$p^L(R_i) = \begin{cases} 1, & R_i \in (0, d] \\ 0, & R_i \in (d, \infty] \end{cases}, \quad (29)$$

where d is a constant distance below which all BSs connect with the typical MU with LOS transmissions. This model has been used in some recent work [7, 9]. With assumptions above,

the intensity measure for NLOS transmissions, i.e., $\Lambda^{\text{NL}}(\cdot)$, is expressed as follows

$$\begin{aligned}
\Lambda^{\text{NL}}([0, t]) &= \mathbb{E}_{\mathcal{H}^{\text{NL}}} \left[2\pi\lambda \int_{R_i=0}^{t(B^{\text{NL}}\mathcal{H}^{\text{NL}})^{1/\alpha^{\text{NL}}}} p^{\text{NL}}(R_i) R_i dR_i \right] \\
&= 2\pi\lambda \int_{\mathcal{H}^{\text{NL}}=0}^{\frac{1}{B^{\text{NL}}}(\frac{d}{t})^{\alpha^{\text{NL}}}} \int_{R_i=0}^{t(B^{\text{NL}}\mathcal{H}^{\text{NL}})^{1/\alpha^{\text{NL}}}} p^{\text{NL}}(R_i) R_i f_{H^{\text{NL}}}(\mathcal{H}^{\text{NL}}) dR_i d\mathcal{H}^{\text{NL}} \\
&\quad + 2\pi\lambda \int_{\mathcal{H}^{\text{NL}}=\frac{1}{B^{\text{NL}}}(\frac{d}{t})^{\alpha^{\text{NL}}}}^{\infty} \int_{R_i=0}^{t(B^{\text{NL}}\mathcal{H}^{\text{NL}})^{1/\alpha^{\text{NL}}}} p^{\text{NL}}(R_i) R_i f_{H^{\text{NL}}}(\mathcal{H}^{\text{NL}}) dR_i d\mathcal{H}^{\text{NL}} \\
&= 0 + 2\pi\lambda \int_{\mathcal{H}^{\text{NL}}=\frac{1}{B^{\text{NL}}}(\frac{d}{t})^{\alpha^{\text{NL}}}}^{\infty} \left[\frac{t^2}{2} (B^{\text{NL}}\mathcal{H}^{\text{NL}})^{2/\alpha^{\text{NL}}} - \frac{d^2}{2} \right] f_{H^{\text{NL}}}(\mathcal{H}^{\text{NL}}) d\mathcal{H}^{\text{NL}} \\
&= \frac{1}{2}\pi\lambda t^2 (B^{\text{NL}})^{2/\alpha^{\text{NL}}} e^{1/M_{\text{NL}}^2} \text{erfc}[M_{\text{NL}} \ln t + Q_{\text{NL}}] \\
&\quad - \frac{1}{2}\pi\lambda d^2 \text{erfc}[M_{\text{NL}} \ln t + V_{\text{NL}}], \tag{30}
\end{aligned}$$

where $\text{erfc}(\cdot)$ is the complementary error function, $M_{\text{NL}} = -\frac{\alpha^{\text{NL}}}{\sqrt{2}\sigma^{\text{NL}}}$, $Q_{\text{NL}} = \frac{\alpha^{\text{NL}} \ln d - \ln B^{\text{NL}}}{\sqrt{2}\sigma^{\text{NL}}} - \frac{1}{M_{\text{NL}}}$ and $V_{\text{NL}} = \frac{\alpha^{\text{NL}} \ln d - \ln B^{\text{NL}}}{\sqrt{2}\sigma^{\text{NL}}}$ are all constants. After obtaining $\Lambda^{\text{NL}}(\cdot)$, the intensity of NLOS BSs, i.e., $\lambda^{\text{NL}}(\cdot)$, can be readily derived as follows

$$\begin{aligned}
\lambda^{\text{NL}}(t) &= \frac{d}{dt} \Lambda^{\text{NL}}([0, t]) \\
&= \pi\lambda t (B^{\text{NL}})^{2/\alpha^{\text{NL}}} e^{1/M_{\text{NL}}^2} \text{erfc}[M_{\text{NL}} \ln t + Q_{\text{NL}}] + \frac{M_{\text{NL}}\lambda\sqrt{\pi}d^2}{t} e^{-(M_{\text{NL}} \ln t + V_{\text{NL}})^2} \\
&\quad - M_{\text{NL}}\lambda t\sqrt{\pi} (B^{\text{NL}})^{2/\alpha^{\text{NL}}} e^{1/M_{\text{NL}}^2 - (M_{\text{NL}} \ln t + Q_{\text{NL}})^2}. \tag{31}
\end{aligned}$$

Similarly, the intensity measure and intensity for LOS BSs are

$$\Lambda^{\text{L}}([0, t]) = \frac{1}{2}\pi\lambda t^2 (B^{\text{L}})^{2/\alpha^{\text{L}}} e^{1/M_{\text{L}}^2} \text{erfc}[M_{\text{L}} \ln t + Q_{\text{L}}] + \frac{1}{2}\pi\lambda d^2 \text{erfc}[-M_{\text{L}} \ln t + V_{\text{L}}], \tag{32}$$

and

$$\begin{aligned}
\lambda^{\text{L}}(t) &= \pi\lambda t (B^{\text{L}})^{2/\alpha^{\text{L}}} e^{1/M_{\text{L}}^2} \text{erfc}[M_{\text{L}} \ln t + Q_{\text{L}}] + \frac{M_{\text{L}}\lambda\sqrt{\pi}d^2}{t} e^{-(-M_{\text{L}} \ln t + V_{\text{L}})^2} \\
&\quad - M_{\text{L}}\lambda t\sqrt{\pi} (B^{\text{L}})^{2/\alpha^{\text{L}}} e^{1/M_{\text{L}}^2 - (M_{\text{L}} \ln t + Q_{\text{L}})^2}, \tag{33}
\end{aligned}$$

respectively, where $M_{\text{L}} = \frac{\alpha^{\text{L}}}{\sqrt{2}\sigma^{\text{L}}}$, $Q_{\text{L}} = \frac{\ln B^{\text{L}} - \alpha^{\text{L}} \ln d}{\sqrt{2}\sigma^{\text{L}}} + \frac{1}{M_{\text{L}}}$ and $V_{\text{L}} = \frac{\alpha^{\text{L}} \ln d - \ln B^{\text{L}}}{\sqrt{2}\sigma^{\text{L}}}$ are all constants. By substituting $\lambda^{\text{NL}}(\cdot)$ and $\lambda^{\text{L}}(\cdot)$ above into Eq. (27) and Eq. (28), the coverage probability

can be obtained in this specific scenario, followed by results in Section VII.

In the above scenario, the shadowing follows log-normal distributions. However, Theorem 7 can also be applied to a generalized shadowing/fading model and the coverage probability with Rayleigh fading will be derived in Section VI.

In the following, an asymptotic analysis will be given for the situation where BS deployment becomes ultra dense, i.e., $\lambda \rightarrow \infty$, which helps to determine boundaries between adjacent regimes.

Corollary 8. *If $T \geq 0$ dB, the coverage probability of $p_c(\lambda, T)$ in Eq. (26) when $\lambda \rightarrow \infty$ converges as follows*

$$\begin{aligned} \lim_{\lambda \rightarrow \infty} p_c(\lambda, T) &= \lim_{\lambda \rightarrow \infty} \Pr[SINR > T] \\ &\stackrel{(a)}{=} \lim_{\lambda \rightarrow \infty} \Pr[SIR > T] \\ &\stackrel{(b)}{=} \frac{\alpha^L \sin(2\pi/\alpha^L)}{2\pi T^{2/\alpha^L}}. \end{aligned} \quad (34)$$

Proof: A sketch of the proof of Corollary 8 is given here. In Eq. (34), (a) is due to the reason that when $\lambda \rightarrow \infty$, the network is interference-limited and noise can be ignored compared with the aggregate interference, which is also validated by results in Section VII. The proof of (b) can be found in [13, Remark 9] and [7, Theorem 4] and are omitted here. ■

From Corollary 8, it can be concluded that for dense SCNs the coverage probability is invariant with respect to BS intensity λ and even the distribution of shadowing/fading.

Finally, the ASE in units of bps/Hz/km² for a given BS intensity λ can be derived as follows

$$\begin{aligned} ASE(\lambda) &= \lambda \mathbb{E}_{SINR} [\log_2(1 + SINR)] \\ &= \lambda \int_{x=0}^{\infty} \log_2(1 + x) f(x) dx \\ &= \lambda \int_{x=0}^{\infty} \int_{y=0}^x \frac{1}{\ln 2 (1 + y)} dy f(x) dx \\ &= \lambda \int_{y=0}^{\infty} \frac{1}{\ln 2 (1 + y)} \int_{x=y}^{\infty} f(x) dx dy \end{aligned}$$

$$= \lambda \int_{y=0}^{\infty} \frac{[1 - F(y)]}{\ln 2 (1 + y)} dy = \frac{\lambda}{\ln 2} \int_{u=0}^{\infty} \frac{p_c(\lambda, u)}{u + 1} du. \quad (35)$$

where $f(x)$ and $F(x)$ are the probability density function (PDF) and CDF of the SINR, respectively.

VI. COMPARISONS WITH OTHER CELL ASSOCIATION SCHEMES

In this section, we will apply Theorem 7 to a SCN with Rayleigh fading. Moreover, the strongest received signal power association scheme is compared with the nearest BS association scheme to evaluate the performance impact of the two different cell association schemes. For brevity, we denote SPAS and NBAS by the strongest power association scheme and the nearest BS association scheme, respectively.

A. Rayleigh Fading Assuming SPAS

As the majority of previous work considered Rayleigh fading and ignored log-normal shadowing, in this part we will apply our proposed model to Rayleigh fading scenario for the sake of a fair comparison. The main difference for theoretical analysis when replacing log-normal shadowing with Rayleigh fading lies in the intensity measure and the intensity. Assuming that \mathcal{H}^{NL} and \mathcal{H}^{L} follow exponential distributions with rates μ^{NL} and μ^{L} , respectively, then $\Lambda^{\text{NL}}(\cdot)$, $\Lambda^{\text{L}}(\cdot)$, $\lambda^{\text{NL}}(\cdot)$, $\lambda^{\text{L}}(\cdot)$ can be calculated based on Theorem 3 as follows

$$\begin{aligned} \Lambda^{\text{NL}}([0, t]) &= 2\pi\lambda \int_{\mathcal{H}^{\text{NL}} = \frac{1}{B^{\text{NL}}} \left(\frac{d}{t}\right)^{\alpha^{\text{NL}}}}^{\infty} \left[\frac{t^2}{2} (B^{\text{NL}} \mathcal{H}^{\text{NL}})^{2/\alpha^{\text{NL}}} - \frac{d^2}{2} \right] f_{\mathcal{H}^{\text{NL}}}(\mathcal{H}^{\text{NL}}) d\mathcal{H}^{\text{NL}} \\ &= \pi\lambda \left(\frac{B^{\text{NL}}}{\mu^{\text{NL}}} \right)^{2/\alpha^{\text{NL}}} t^2 \Gamma \left(\frac{2}{\alpha^{\text{NL}}} + 1, \frac{\mu^{\text{NL}}}{B^{\text{NL}}} \left(\frac{d}{t} \right)^{\alpha^{\text{NL}}} \right) - \pi\lambda d^2 e^{-\frac{\mu^{\text{NL}}}{B^{\text{NL}}} \left(\frac{d}{t}\right)^{\alpha^{\text{NL}}}}, \end{aligned} \quad (36)$$

$$\lambda^{\text{NL}}(t) \frac{d}{dt} \Lambda^{\text{NL}}([0, t]) = 2\pi\lambda t \left(\frac{B^{\text{NL}}}{\mu^{\text{NL}}} \right)^{2/\alpha^{\text{NL}}} \Gamma \left(\frac{2}{\alpha^{\text{NL}}} + 1, \frac{\mu^{\text{NL}}}{B^{\text{NL}}} \left(\frac{d}{t} \right)^{\alpha^{\text{NL}}} \right), \quad (37)$$

$$\Lambda^{\text{L}}([0, t]) = \pi\lambda t^2 \left(\frac{B^{\text{L}}}{\mu^{\text{L}}} \right)^{2/\alpha^{\text{L}}} \gamma \left(\frac{2}{\alpha^{\text{L}}} + 1, \frac{\mu^{\text{L}}}{B^{\text{L}}} \left(\frac{d}{t} \right)^{\alpha^{\text{L}}} \right) + \pi\lambda d^2 e^{-\frac{\mu^{\text{L}}}{B^{\text{L}}} \left(\frac{d}{t}\right)^{\alpha^{\text{L}}}}, \quad (38)$$

and

$$\lambda^{\text{L}}(t) = \frac{d}{dt} \Lambda^{\text{L}}([0, t]) = 2\pi\lambda t \left(\frac{B^{\text{L}}}{\mu^{\text{L}}} \right)^{2/\alpha^{\text{L}}} \gamma \left(\frac{2}{\alpha^{\text{L}}} + 1, \frac{\mu^{\text{L}}}{B^{\text{L}}} \left(\frac{d}{t} \right)^{\alpha^{\text{L}}} \right), \quad (39)$$

where $\Gamma(s, x) = \int_x^\infty v^{s-1} e^{-v} dv$ and $\gamma(s, x) = \int_0^x v^{s-1} e^{-v} dv$ denote the upper and the lower incomplete gamma functions, respectively, $\Gamma(s) = \int_0^\infty v^{s-1} e^{-v} dv$ is the gamma function.

By incorporating Eq. (36) - (39) into Eq. (26), the coverage probability of a SCN experiencing Rayleigh fading while using SPAS can be calculated. We omit the rest of derivations for brevity.

B. Rayleigh Fading Assuming NBAS

In this part, the coverage probability will be provided by applying NBAS. Two scenarios will be considered, i.e., with consideration of NLOS and LOS transmissions and without considering the coexistence of NLOS and LOS transmissions, for comparisons with SPAS.

With consideration of NLOS and LOS transmissions: The derivations are very similar to the work in [25] and we just present the results as follows

$$\begin{aligned}
p_c(\lambda, T) &= p_c^L(\lambda, T) + p_c^{\text{NL}}(\lambda, T) \\
&= \int_{r=0}^d 2\pi\lambda r e^{-\frac{T r \eta^{\alpha^L}}{\mu^L B^L} - \pi\lambda r^2} \exp \left[\int_{u=r}^d \frac{-2\pi\lambda T u}{T + \left(\frac{u}{r}\right)^{\alpha^L}} du + \int_{u=d}^\infty \frac{-2\pi\lambda T u}{T + \frac{\mu^L B^L u^{\alpha^{\text{NL}}}}{\mu^{\text{NL}} B^{\text{NL}} r^{\alpha^L}}} du \right] dr \\
&\quad + \int_{r=d}^\infty 2\pi\lambda r e^{-\frac{T r \eta^{\alpha^{\text{NL}}}}{\mu^{\text{NL}} B^{\text{NL}}} - \pi\lambda r^2} \exp \left[\int_{u=0}^d \frac{-2\pi\lambda T u}{T + \left(\frac{u}{r}\right)^{\alpha^{\text{NL}}}} du \right] dr. \tag{40}
\end{aligned}$$

Without considering the coexistence of NLOS and LOS transmissions: If we do not differentiate NLOS and LOS transmissions, the coverage probability using NBAS is given in [12, Theorem 2] as follows

$$p_c(\lambda, T) = \pi\lambda \int_{r=0}^\infty e^{-\pi\lambda r[1+\rho(T)] - \mu^U T \eta^{\alpha^U/2}/B^U} dr, \tag{41}$$

where $U \in \{\text{NL}, \text{L}\}$ and $\rho(T) = T^{2/\alpha^U} \int_{u=T-2/\alpha^U}^\infty \frac{1}{1+u^{\alpha^U/2}} du$

VII. SIMULATIONS AND DISCUSSIONS

This section presents numerical results to validate our analysis, followed by discussions to shed new light on the performance of the SCNs. We use the following parameter values, $P_t = 30$ dBm, $A^{\text{NL}} = 30.8$ dB, $A^{\text{L}} = 2.7$ dB, $\sigma^{\text{NL}} = 4.28$, $\sigma^{\text{L}} = 2.42$, $\mu^{\text{NL}} = \frac{1}{23.45}$,

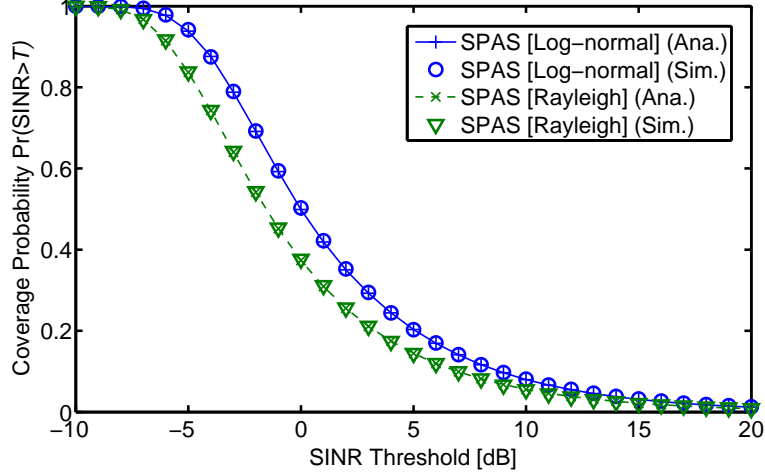


Figure 2. Coverage probability vs. SINR threshold assuming SPAS, $\lambda = 100$ BSs/km².

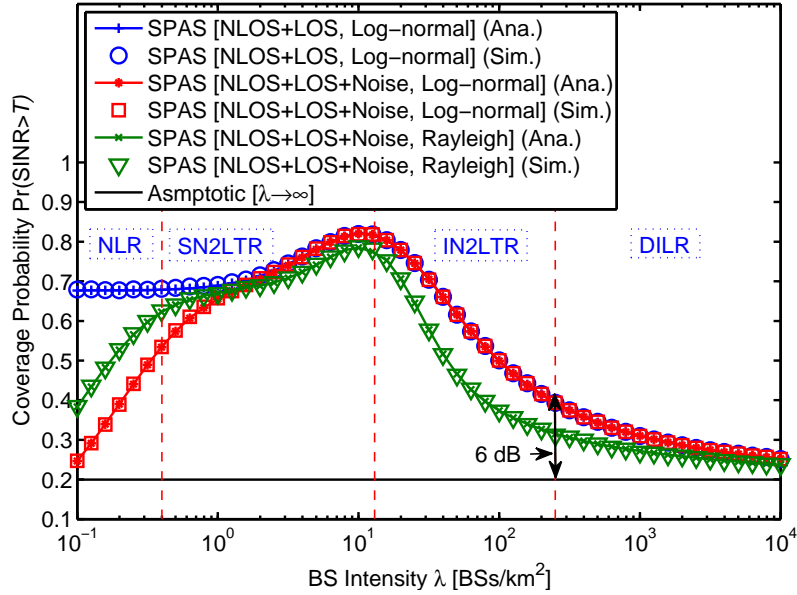


Figure 3. Coverage probability vs. BS intensity λ , $T = 0$ dB.

$$\mu^L = \frac{1}{7.32}, \sigma^{\text{NL}} = 4 \text{ dB}, \sigma^L = 3 \text{ dB}, \eta = -95 \text{ dBm}^3, T = 0 \text{ dB} \text{ and } d = 250 \text{ m} [7, 9, 18].$$

A. Validation of the Analytical Results of $p_c(\lambda, T)$ with Monte Carlo Simulations

Fig. 2 illustrates the coverage probability with respect to different SINR thresholds. We can observe that the analytical results (solid lines or dash lines) match well with the simulation

²The mean of Rayleigh fading for NLOS (or LOS) transmissions is equal to the mean of log-normal shadowing for NLOS (or LOS) transmissions.

³Including a noise figure of 9 dB at the typical MU.

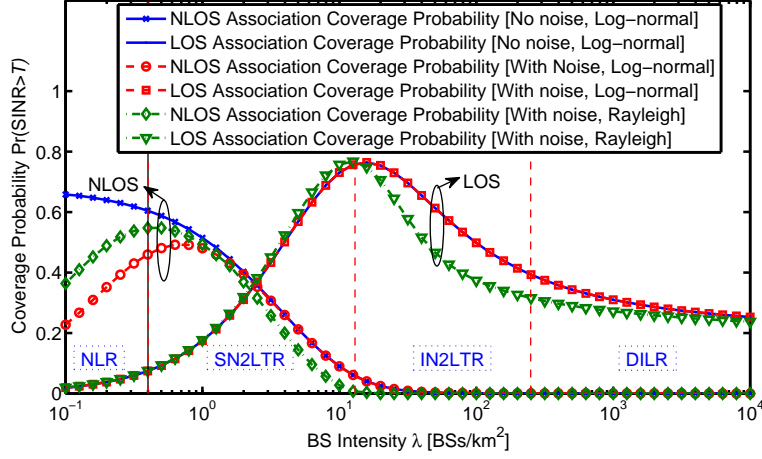


Figure 4. NLOS/LOS association coverage probability vs. BS intensity λ assuming SPAS, $T = 0$ dB.

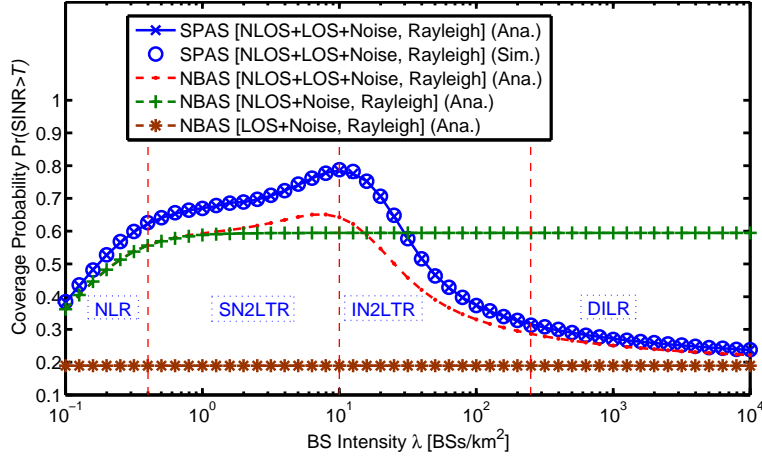


Figure 5. Comparison of different cell association schemes, i.e., SPAS and NBAS, , $T = 0$ dB.

results (markers), which validate our analytical analysis. The coverage probability decrease with the increase of SINR threshold, which is intuitively correct as a higher SINR threshold requires a higher signal quality. We also plot figures adopting different shadowing/fading models, i.e., log-normal shadowing and Rayleigh fading.

To fully study the SINR coverage probability with respect to BS intensity, the results of $p_c(\lambda, T)$ configured with $T = 0$ dB and assuming SPAS are plotted in Fig. 3 and Fig. 4. As can be observed from Fig. 3, the analytical results match the simulation results well with respect to various BS intensities λ from 10^{-1} BSs/km² to 10^4 BSs/km². With the assistance of Fig. 4, we conclude that the performance of small cell networks can be divided into four different regimes according to the intensity of small cell BSs, where in each regime, the

performance is dominated by different factors.

- **Noise-Limited Regime (NLR):** ($\lambda \leq 0.4$ BSs/km² in Fig. (3) and using the parameters in the simulation). In this regime, the typical MU is likely to have a NLOS path with the serving BS. The network in the NLR regime is very sparse and thus the interference can be ignored compared with the thermal noise if we use **SINR** for performance metric. In this case, $\text{SINR} = \frac{S}{\eta}$ and the coverage probability will increase with the increase of λ as the strongest received power (S) will grow and noise power (η) will remain the same. While if we use **SIR** for performance metric, the SIR coverage probability remain almost stable in this regime as λ increases. This is because the increase in the received signal power is counterbalanced by the increase in the aggregate interference power. Besides, as the aggregate interference power is smaller than noise power, the SIR coverage probability is larger than the SINR coverage probability.
- **Signal NLOS-to-LOS-Transition Regime (SN2LTR):** ($\lambda \in (0.4, 13]$ BSs/km² in Fig. (3) and using the parameters in the simulation). In this regime, when λ is small, the typical MU has a higher probability to connect to a NLOS BS; while when λ becomes larger, the typical MU has an increasingly higher probability to connect to a LOS BS. That is to say, with the increase of λ , the typical MU is more likely to be in LOS with the associated BS, i.e., the received signal transforms from NLOS to LOS path. Even though the associated BS is LOS, the majority of interfering BSs are still NLOS in this regime and thus the SINR (or SIR) coverage probability keeps growing. Besides, from this regime on, noise power has a negligible impact on coverage performance, i.e., the SCN is interference-limited.
- **Interference NLOS-to-LOS-Transition Regime (IN2LTR):** ($\lambda \in (13, 250]$ BSs/km² in Fig. (3) and using the parameters in the simulation). In this regime, the typical MU is connected to a LOS BS with a high probability. However, different from the situation in the SN2LTR, the majority of interfering BSs experience transitions from NLOS to LOS path, which causes much more severe interference to the typical MU compared with NLOS interfering BSs. As a result, the SINR (or SIR) coverage probability decreases as the increase of λ because the transition of interference from NLOS path to LOS path

causes a larger increase in interference compared with that in signal.

- **Dense Interference-Limited Regime (DILR):** ($\lambda > 250$ BSs/km² in Fig. (3) and using the parameters in the simulation). In this regime, the network is extremely dense and grow close to the LOS-BS-only scenario as the increase of λ . The SINR (or SIR) coverage probability will become stable with the increase in BS intensity as any increase in the received LOS BS signal power is counterbalanced by the increase in the aggregate LOS BS interference power, which is also illuminated by Corollary 8.

Remark 9. Note that the boundaries between two adjacent regimes are quite *qualitative* which are worth further investigation. When different sets of parameters are considered, the boundaries may change. However the main conclusion obtained will hold, i.e., the performance can be divided into four different regimes and in each regimes the performance is dominated by different factors.

Another interesting observation in Fig. 3 is that the network experiencing Rayleigh fading outperforms that experiencing log-normal shadowing when the network is sparse, while the network experiencing log-normal shadowing outperforms that experiencing Rayleigh fading when the SCN becomes dense. However, this phenomenon is highly related to the assumed SINR threshold, which is shown in Fig. 2. If the SCN becomes ultra dense, the coverage probability approaches the same asymptotic value regardless of shadowing or fading model.

In Fig. 5, we compare the performance of different cell association schemes using NBAS as a baseline. To guarantee the fairness of comparison, Rayleigh fading is assumed for all studied scenarios. It is observed that by assuming SPAS, the coverage probability have a considerable gain compared with that assuming NBAS, with the peak coverage probability rising from 0.6 to 0.8. Besides, we also plot figures which are exclusive of NLOS/LOS transmissions, i.e., signal-slope path loss model [12] is adopted. It is found that the coverage probability firstly increase with the increase of BS intensity λ and then becomes stable and independent of λ when the SCN is dense, if we adopt parameters of NLOS transmissions to the signal-slope path loss model. In comparison, the coverage probability is stable even when the BS intensity is rather sparse, if we adopt parameters of LOS transmissions to the signal-slope path loss model.

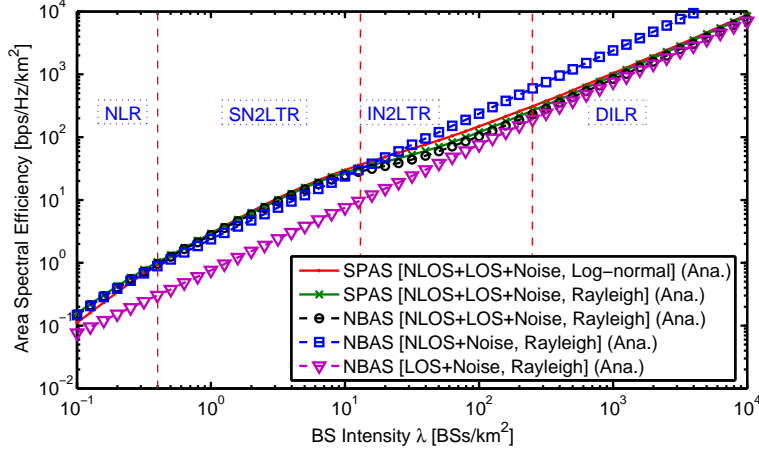


Figure 6. The area spectral efficiency vs. BS intensity λ , $T = 0$ dB.

B. Discussion on the Analytical Results of ASE (λ)

In this part, the ASE with $T = 0$ dB is evaluated analytically only, as ASE (λ) is a function of $p_c(\lambda, T)$ shown in Eq. (35).

Fig. 6 illustrates the ASE with different cell association schemes vs. BS intensity λ . It is found that the ASE of the sparse SCN has a similar growth tendency with that of the SCN which employs NLOS transmission configurations, while the ASE of dense SCN approaches the performance of the SCN which employs LOS transmission configurations. Specifically, when the SCN is in the NLR and SN2LTR, e.g., $\lambda \leq 13$ BSs/km², the ASE quickly increases with λ because the network is generally noise-limited or the aggregate interference power is relatively low, and thus adding more small cells immensely benefits the ASE of the SCN. And when the network is in the front section of IN2LTR, i.e., $\lambda \in [13, 100]$ BSs/km², the ASE exhibits a slowing-down in the rate of growth due to the fast decrease of the coverage probability at $\lambda \in [13, 100]$ BSs/km², which is shown in Fig. 3, Fig. 4 and Fig. 5. Second, when $\lambda \geq 100$ BSs/km², the ASE will pick up the growth rate since the decrease of the coverage probability becomes a minor factor compared with the increase of BS intensity λ . Finally, when the SCN becomes extremely dense, i.e., in the DILR, the ASE exhibits a nearly linear trajectory with regard to λ because both the signal power and the interference power are now LOS dominated, and thus statistically stable as explained before.

VIII. CONCLUSIONS AND FUTURE WORK

In this paper, we proposed a unified framework to analyze the performance of the SCNs in terms of the coverage probability and the ASE. In our analysis, we considered a practical path loss model that accounted for NLOS and LOS transmissions. Furthermore, we adopted a generalized shadowing/fading model, in which log-normal shadowing and/or Rayleigh fading could be treated in a unified framework. The cell association scheme adopted is based on the strongest received signal power, which has been widely used in practice but rarely considered in analytical studies due to the difficulty in the theoretical analysis. The coverage probability and the ASE were derived, using a generalized stochastic geometry analysis based on a transformed PPP using the Equivalence theorem. Using the analysis, we showed for the first time that depending on the intensity of the BSs, the performance of the SCNs can be divided into four different regimes, i.e., the noise-limited regime, the signal NLOS-to-LOS-transition regime, the interference NLOS-to-LOS-transition regime and the dense interference-limited regime, where in each regime the performance is dominated by different factors. The analysis helps to understand as the intensity of the BSs grows continually, which dominant factor that determines the cellular network performance and therefore provide guidance on the design and management of the cellular networks as we evolve into dense SCNs. Moreover, the strongest received signal power association scheme leads to larger SINR (or SIR) coverage probability and ASE compared with the nearest BS association scheme in the SCNs.

In our future work, shadowing and multi-path fading model will be considered simultaneously which is more practical for the real network. Furthermore, heterogeneous networks incorporating both NLOS and LOS transmissions will also be investigated.

APPENDIX A: PROOF OF THEOREM 3

Firstly, we will obtain the intensity measure Λ^{NL} of $\overline{\Phi^{\text{NL}}}$; and then the intensity λ^{NL} will be easily acquired by taking a derivation of Λ^{NL} . By using displacement theorem [13, 24],

the point process $\overline{\Phi}^{\text{NL}}$ is Poisson with intensity measure

$$\begin{aligned}
\Lambda^{\text{NL}}([0, t]) &= \mathbb{E}_{\overline{\Phi}^{\text{NL}}} [b(0, t)] \\
&= \int_{\mathbb{R}^2} \Pr [\bar{R}_i < t] p^{\text{NL}}(R_i) \lambda d\mathbf{X}_i \\
&= \mathbb{E}_{\mathcal{H}^{\text{NL}}} \left\{ \int_{\mathbb{R}^2} \Pr \left[(B^{\text{NL}} \mathcal{H}^{\text{NL}})^{-1/\alpha^{\text{NL}}} R_i < t \right] p^{\text{NL}}(R_i) \lambda d\mathbf{X}_i \right\} \\
&= \mathbb{E}_{\mathcal{H}^{\text{NL}}} \left\{ \int_{\mathbb{R}^2} \Pr \left[R_i < t (B^{\text{NL}} \mathcal{H}^{\text{NL}})^{1/\alpha^{\text{NL}}} \right] p^{\text{NL}}(R_i) \lambda d\mathbf{X}_i \right\} \\
&\stackrel{(a)}{=} \mathbb{E}_{\mathcal{H}^{\text{NL}}} \left[\int_{\theta=0}^{2\pi} \int_{R_i=0}^{t(B^{\text{NL}} \mathcal{H}^{\text{NL}})^{1/\alpha^{\text{NL}}}} p^{\text{NL}}(R_i) \lambda R_i dR_i d\theta \right] \\
&= \mathbb{E}_{\mathcal{H}^{\text{NL}}} \left[2\pi \lambda \int_{R_i=0}^{t(B^{\text{NL}} \mathcal{H}^{\text{NL}})^{1/\alpha^{\text{NL}}}} p^{\text{NL}}(R_i) R_i dR_i \right], \tag{42}
\end{aligned}$$

where $b(0, t)$ is a ball centered at the origin o with radius t and (a) results by converting from Cartesian to polar coordinates. Then the intensity of $\overline{\Phi}^{\text{NL}}$ denoted by $\lambda^{\text{NL}}(\cdot)$ can be given by

$$\lambda^{\text{NL}}(t) = \frac{d}{dt} \Lambda^{\text{NL}}([0, t]). \tag{43}$$

Note that to ensure the intensity measure is finite for any bounded set (a set is bounded if it can be contained in a ball with a finite radius), \mathcal{H}^{NL} has to satisfy a certain condition. As $p^{\text{NL}}(R_i) \leq 1$, from Eq. (42), we get an inequality as follows

$$\begin{aligned}
\Lambda^{\text{NL}}([0, t]) &= \mathbb{E}_{\mathcal{H}^{\text{NL}}} \left[2\pi \lambda \int_{R_i=0}^{t(B^{\text{NL}} \mathcal{H}^{\text{NL}})^{1/\alpha^{\text{NL}}}} p^{\text{NL}}(R_i) R_i dR_i \right] \\
&\leq \mathbb{E}_{\mathcal{H}^{\text{NL}}} \left[2\pi \lambda \int_{R_i=0}^{t(B^{\text{NL}} \mathcal{H}^{\text{NL}})^{1/\alpha^{\text{NL}}}} R_i dR_i \right] \\
&= \pi \lambda t^2 (B^{\text{NL}})^{2/\alpha^{\text{NL}}} \mathbb{E}_{\mathcal{H}^{\text{NL}}} \left[(\mathcal{H}^{\text{NL}})^{2/\alpha^{\text{NL}}} \right]. \tag{44}
\end{aligned}$$

If the expectation $\mathbb{E}_{\mathcal{H}^{\text{NL}}} \left[(\mathcal{H}^{\text{NL}})^{2/\alpha^{\text{NL}}} \right] < \infty$, then $\Lambda^{\text{NL}}([0, t]) < \infty$. Using similar approach, the intensity measure and intensity of the PPP $\overline{\Phi}^{\text{L}}$ are obtained by Eq. (18) and Eq. (16), respectively.

As for the cell association scheme, it is obvious that the original scheme $(\mathbf{X}_i, \mathbf{U})^* =$

$\arg \max_{(\mathbf{X}_i, \mathbf{U}) \in \mathbb{S}} B^{\mathbf{U}} \mathcal{H}^{\mathbf{U}} (R_i)^{-\alpha^{\mathbf{U}}}$ is equivalent to the scheme $(\mathbf{X}_i, \mathbf{U})^* = \arg \max_{(\mathbf{X}_i, \mathbf{U}) \in \mathbb{S}} (\overline{R}_i)^{-\alpha^{\mathbf{U}}}$ which actually corresponds to the nearest BS association scheme. Thus the proof is completed.

APPENDIX B: PROOF OF LEMMA 6

Denote the strongest NLOS received signal power and the strongest LOS received signal power by \mathcal{P}^{NL} and \mathcal{P}^{L} , respectively. That is, $\mathcal{P}^{\text{NL}} = \max(P_i^{\text{NL}})$ and $\mathcal{P}^{\text{L}} = \max(P_i^{\text{L}})$. Then the probability $\Pr[\mathcal{P} \leq \gamma]$ can be derived as

$$\begin{aligned}
\Pr[\mathcal{P} \leq \gamma] &= \Pr \left[\max \left(\overline{R}_i^{\text{NL}}^{-\alpha^{\text{NL}}} \right) \leq \gamma \cap \max \left(\overline{R}_i^{\text{L}}^{-\alpha^{\text{L}}} \right) \leq \gamma \right] \\
&= \Pr \left[\min \left(\overline{R}_i^{\text{NL}} \right) \geq \gamma^{-1/\alpha^{\text{NL}}} \cap \min \left(\overline{R}_i^{\text{L}} \right) \geq \gamma^{-1/\alpha^{\text{L}}} \right] \\
&= \Pr \left[\text{no nodes within } \gamma^{-1/\alpha^{\text{NL}}} \cap \text{no nodes within } \gamma^{-1/\alpha^{\text{L}}} \right] \\
&= \Pr \left[\overline{\Phi}^{\text{NL}} \left(b \left(0, \gamma^{-1/\alpha^{\text{NL}}} \right) \right) = 0 \cap \overline{\Phi}^{\text{L}} \left(b \left(0, \gamma^{-1/\alpha^{\text{L}}} \right) \right) = 0 \right] \\
&\stackrel{(a)}{=} \Pr \left[\overline{\Phi}^{\text{NL}} \left(b \left(0, \gamma^{-1/\alpha^{\text{NL}}} \right) \right) = 0 \right] \cdot \Pr \left[\overline{\Phi}^{\text{L}} \left(b \left(0, \gamma^{-1/\alpha^{\text{L}}} \right) \right) = 0 \right] \\
&\stackrel{(b)}{=} \exp \left[-\Lambda^{\text{NL}} \left(\left[0, \gamma^{-1/\alpha^{\text{NL}}} \right] \right) \right] \cdot \exp \left[-\Lambda^{\text{L}} \left(\left[0, \gamma^{-1/\alpha^{\text{L}}} \right] \right) \right], \tag{45}
\end{aligned}$$

where the notation $\overline{\Phi}^{\mathbf{U}}(\Xi)$ refers to the number of points $x \in \overline{\Phi}^{\mathbf{U}}$ contained in the set Ξ , while equality (a) follows from the independence of PPP $\overline{\Phi}^{\text{NL}}$ and PPP $\overline{\Phi}^{\text{L}}$, and (b) comes from the fact that the void probability $\Pr \left[\overline{\Phi}^{\mathbf{U}}(b(0, r)) = 0 \right] = \exp[-\Lambda^{\mathbf{U}}([0, r])]$ for a non-homogeneous PPP. Then the rest of the proof is straightforward.

APPENDIX C: PROOF OF THEOREM 7

By invoking the law of total probability, the coverage probability can be divided into two parts, i.e., $p_c^{\text{NL}}(\lambda, T)$ and $p_c^{\text{L}}(\lambda, T)$, which denotes the conditional coverage probability given that the typical MU is associated with a BS in Φ^{NL} and Φ^{L} , respectively. Moreover, denote by \mathcal{P}^{NL} and \mathcal{P}^{L} the strongest received signal power from BS in Φ^{NL} and Φ^{L} , i.e., $\mathcal{P}^{\text{NL}} = \max(P_i^{\text{NL}})$ and $\mathcal{P}^{\text{L}} = \max(P_i^{\text{L}})$, respectively. Then by applying the law of total

probability, $p_c^L(\lambda, T)$ can be computed by

$$\begin{aligned} p_c^L(\lambda, T) &= \Pr [(\text{SINR}^L > T) \cap (\mathcal{P}^L > \mathcal{P}^{\text{NL}}) \cap \mathcal{Y}^L] \\ &= \mathbb{E}_{\mathcal{Y}^L} \left\{ \underbrace{\Pr [\text{SINR}^L > T | (\mathcal{P}^L > \mathcal{P}^{\text{NL}}) \cap \mathcal{Y}^L]}_{\text{II}} \cdot \underbrace{\Pr [\mathcal{P}^L > \mathcal{P}^{\text{NL}} | \mathcal{Y}^L]}_{\text{I}} \right\}, \end{aligned} \quad (46)$$

where \mathcal{Y}^L is the equivalent distance between the typical MU and the BS providing the strongest received signal power to the typical MU in Φ^L , i.e., $\mathcal{Y}^L = \arg \max_{\overline{R}_i^L \in \Phi^L} (\overline{R}_i^L)^{-\alpha^L}$, and also note that $\mathcal{P}^L = (\mathcal{Y}^L)^{-\alpha^L}$. Besides, Part I guarantees that the typical MU is connected to a LOS BS and Part II denotes the coverage probability conditioned on the proposed cell association scheme in Eq. (10). Next, Part I and Part II will be respectively derived as follows.

For Part I,

$$\begin{aligned} &\Pr [\mathcal{P}^L > \mathcal{P}^{\text{NL}} | \mathcal{Y}^L] \\ &= \Pr [(\mathcal{Y}^L)^{-\alpha^L} > (\mathcal{Y}^{\text{NL}})^{-\alpha^{\text{NL}}} | \mathcal{Y}^L] \\ &= \Pr [\mathcal{Y}^{\text{NL}} > (\mathcal{Y}^L)^{\alpha^L/\alpha^{\text{NL}}} | \mathcal{Y}^L] \\ &\stackrel{(a)}{=} \exp \left[-\Lambda^{\text{NL}} \left(\left[0, (\mathcal{Y}^L)^{\alpha^L/\alpha^{\text{NL}}} \right] \right) \right], \end{aligned} \quad (47)$$

where \mathcal{Y}^{NL} , similar to the definition of \mathcal{Y}^L , is the equivalent distance between the typical MU and the BS providing the strongest received signal power to the typical MU in Φ^{NL} , i.e., $\mathcal{Y}^{\text{NL}} = \arg \max_{\overline{R}_i^{\text{NL}} \in \Phi^{\text{NL}}} (\overline{R}_i^{\text{NL}})^{-\alpha^{\text{NL}}}$, and also note that $\mathcal{P}^{\text{NL}} = (\mathcal{Y}^{\text{NL}})^{-\alpha^{\text{NL}}}$, and (a) follows from the void probability of a PPP.

For Part II, we know that $\text{SINR} = \frac{\mathcal{P}}{I+\eta} = \frac{\mathcal{P}}{I^{\text{NL}}+I^L+\eta}$, where I^{NL} and I^L denote the aggregate interference from NLOS BSs and LOS BSs, respectively. The conditional coverage probability is derived as follows

$$\begin{aligned} &\Pr [\text{SINR}^L > T | (\mathcal{P}^L > \mathcal{P}^{\text{NL}}) \cap \mathcal{Y}^L] \\ &= \Pr \left[\frac{1}{\text{SINR}^L} < \frac{1}{T} \middle| (\mathcal{P}^L > \mathcal{P}^{\text{NL}}) \cap \mathcal{Y}^L \right] \end{aligned}$$

$$\begin{aligned}
&\stackrel{(a)}{=} \int_{x=0}^{1/T} \int_{\omega=-\infty}^{\infty} \frac{e^{-j\omega x}}{2\pi} \mathcal{F}_{\frac{1}{\text{SINR}^L}}(\omega) d\omega dx \\
&= \int_{\omega=-\infty}^{\infty} \left[\frac{1 - e^{-j\omega/T}}{2\pi j\omega} \right] \mathcal{F}_{\frac{1}{\text{SINR}^L}}(\omega) d\omega,
\end{aligned} \tag{48}$$

where SINR^L denotes the SINR when the typical MU is associated with a LOS BS, the inner integral in (a) is the conditional PDF of $\frac{1}{\text{SINR}^L}$, and $\mathcal{F}_{\frac{1}{\text{SINR}^L}}(\omega)$ denotes the conditional characteristic function of $\frac{1}{\text{SINR}^L}$ which is given by

$$\begin{aligned}
\mathcal{F}_{\frac{1}{\text{SINR}^L}}(\omega) &= \mathbb{E}_{\Phi} \left[\exp \left(j\omega \frac{1}{\text{SINR}^L} \right) \middle| (\mathcal{P}^L > \mathcal{P}^{\text{NL}}) \cap \mathcal{Y}^L \right] \\
&= \mathbb{E}_{\Phi} \left[\exp \left(j\omega \frac{I^{\text{NL}} + I^L + \eta}{\mathcal{P}^L} \right) \middle| (\mathcal{P}^L > \mathcal{P}^{\text{NL}}) \cap \mathcal{Y}^L \right] \\
&= \mathbb{E}_{\Phi} \left\{ \exp \left[j\omega (I^{\text{NL}} + I^L + \eta) (\mathcal{Y}^L)^{\alpha^L} \right] \middle| (\mathcal{P}^L > \mathcal{P}^{\text{NL}}) \cap \mathcal{Y}^L \right\} \\
&\stackrel{(a)}{=} e^{j\omega\eta(\mathcal{Y}^L)^{\alpha^L}} \underbrace{\mathbb{E}_{\Phi^{\text{NL}}} \left\{ \exp \left[j\omega I^{\text{NL}} \cdot (\mathcal{Y}^L)^{\alpha^L} \right] \middle| (\mathcal{P}^L > \mathcal{P}^{\text{NL}}) \cap \mathcal{Y}^L \right\}}_{\text{III}} \\
&\quad \times \underbrace{\mathbb{E}_{\Phi^L} \left\{ \exp \left[j\omega I^L \cdot (\mathcal{Y}^L)^{\alpha^L} \right] \middle| (\mathcal{P}^L > \mathcal{P}^{\text{NL}}) \cap \mathcal{Y}^L \right\}}_{\text{IV}},
\end{aligned} \tag{49}$$

where (a) comes from the facts that $\Phi = \Phi^{\text{NL}} \cup \Phi^L$ and the mutual independence of Φ^{NL} and Φ^L . Now by applying stochastic geometry, we will derive the term III in Eq. (49) as follows

$$\begin{aligned}
&\mathbb{E}_{\Phi^{\text{NL}}} \left\{ \exp \left[j\omega I^{\text{NL}} \cdot (\mathcal{Y}^L)^{\alpha^L} \right] \middle| (\mathcal{P}^L > \mathcal{P}^{\text{NL}}) \cap \mathcal{Y}^L \right\} \\
&\stackrel{(a)}{=} \mathbb{E}_{\overline{\Phi}^{\text{NL}}} \left\{ \exp \left[j\omega \cdot (\mathcal{Y}^L)^{\alpha^L} \sum_{i: \overline{R}_i^{\text{NL}} \in \overline{\Phi}^{\text{NL}'}} \left(\overline{R}_i^{\text{NL}} \right)^{-\alpha^{\text{NL}}} \right] \middle| (\mathcal{P}^L > \mathcal{P}^{\text{NL}}) \cap \mathcal{Y}^L \right\} \\
&\stackrel{(b)}{=} \mathbb{E}_{\overline{\Phi}^{\text{NL}}} \left\{ \prod_{i: \overline{R}_i^{\text{NL}} \in \overline{\Phi}^{\text{NL}'}} \exp \left[j\omega \cdot (\mathcal{Y}^L)^{\alpha^L} \left(\overline{R}_i^{\text{NL}} \right)^{-\alpha^{\text{NL}}} \right] \middle| (\mathcal{P}^L > \mathcal{P}^{\text{NL}}) \cap \mathcal{Y}^L \right\} \\
&\stackrel{(c)}{=} \exp \left\{ \int_{t=(\mathcal{Y}^L)^{\alpha^L/\alpha^{\text{NL}}}}^{\infty} \left[e^{j\omega(\mathcal{Y}^L)^{\alpha^L} t^{-\alpha^{\text{NL}}}} - 1 \right] \lambda^{\text{NL}}(t) dt \right\},
\end{aligned} \tag{50}$$

where in (a), $\overline{\Phi}^{\text{NL}'} = \overline{\Phi}^{\text{NL}} \setminus b \left(0, (\mathcal{Y}^L)^{\alpha^L/\alpha^{\text{NL}}} \right)$ and $\overline{R}_i^{\text{NL}} \in \overline{\Phi}^{\text{NL}'}$ can guarantee the condition that $\mathcal{P}^L > \mathcal{P}^{\text{NL}}$, (b) follows from rewriting the exponential of summation as a product of several exponential functions, and (c) is obtained by applying the probability generating functional

(PGFL) [12, Eq. (3)] of the PPP. Similarly, the term IV in Eq. (49) is given by

$$\begin{aligned}
& \mathbb{E}_{\Phi^L} \left\{ \exp \left[j\omega I^L \cdot (\mathcal{Y}^L)^{\alpha^L} \right] \middle| (\mathcal{P}^L > \mathcal{P}^{\text{NL}}) \cap \mathcal{Y}^L \right\} \\
& \stackrel{(a)}{=} \mathbb{E}_{\overline{\Phi}^L} \left\{ \exp \left[j\omega \cdot (\mathcal{Y}^L)^{\alpha^L} \sum_{i: \overline{R}_i^L \in \overline{\Phi}^L} (\overline{R}_i^L)^{-\alpha^L} \right] \middle| (\mathcal{P}^L > \mathcal{P}^{\text{NL}}) \cap \mathcal{Y}^L \right\} \\
& = \mathbb{E}_{\overline{\Phi}^L} \left\{ \prod_{i: \overline{R}_i^L \in \overline{\Phi}^L} \exp \left[j\omega \cdot (\mathcal{Y}^L / \overline{R}_i^L)^{\alpha^L} \right] \middle| (\mathcal{P}^L > \mathcal{P}^{\text{NL}}) \cap \mathcal{Y}^L \right\} \\
& = \exp \left\{ \int_{t=\mathcal{Y}^L}^{\infty} \left[e^{j\omega (\mathcal{Y}^L/t)^{\alpha^L}} - 1 \right] \lambda^L(t) dt \right\}, \tag{51}
\end{aligned}$$

where in (a), $\overline{\Phi}^L = \overline{\Phi}^L \setminus b(0, \mathcal{Y}^L)$ and $\overline{R}_i^L \in \overline{\Phi}^L$ can guarantee that the typical MU is associated with a LOS BS providing the strongest received signal power. Then the product of Part I and Part II in Eq. (46) can be obtained by substituting them with Eq. (47) – (51).

Finally, note that the value of $p_c^L(\lambda, T)$ in Eq. (46) should be calculated by taking the expectation with respect to \mathcal{Y}^L in terms of its PDF, which is given as follows

$$\begin{aligned}
f_{\mathcal{Y}^L}(y) &= \frac{d}{dy} [1 - \Pr(\mathcal{Y}^L > y)] \\
&= \frac{d}{dy} \{1 - \exp[-\Lambda^L([0, y])]\} \\
&= \exp[-\Lambda^L([0, y])] \cdot \frac{d}{dy} \Lambda^L([0, y]) \\
&= \lambda^L(y) \exp[-\Lambda^L([0, y])]. \tag{52}
\end{aligned}$$

Given that the typical MU is connected to a NLOS BS, the conditional coverage probability $p_c^{\text{NL}}(\lambda, T)$ can be derived in a similar way as the above. In this way, the coverage probability is obtained by $p_c(\lambda, T) = p_c^L(\lambda, T) + p_c^{\text{NL}}(\lambda, T)$. Thus the proof is completed.

REFERENCES

- [1] J. G. Andrews, S. Buzzi, C. Wan, S. V. Hanly, A. Lozano, A. C. K. Soong, and J. C. Zhang, “What will 5g be?” *IEEE J. Sel. Areas Commun.*, vol. 32, no. 6, pp. 1065–1082, Jun. 2014.
- [2] Cisco, “Global mobile data traffic forecast update, 2015-2020,” *Cisco white paper*, Feb. 2016.
- [3] D. Lopez-Perez, M. Ding, H. Claussen, and A. H. Jafari, “Towards 1 gbps/ue in cellular systems: Understanding ultra-dense small cell deployments,” *IEEE Commun. Surv. Tut.*, vol. 17, no. 4, pp. 2078–2101, Nov. 2015.

- [4] X. Ge, S. Tu, G. Mao, C. X. Wang, and T. Han, "5g ultra-dense cellular networks," *IEEE Wireless Commun.*, vol. 23, no. 1, pp. 72–79, Feb. 2016.
- [5] X. Ge, S. Tu, T. Han, Q. Li, and G. Mao, "Energy efficiency of small cell backhaul networks based on gauss-markov mobile models," *IET Networks*, vol. 4, no. 2, pp. 158–167, Mar. 2015.
- [6] M. Ding, P. Wang, D. Lopez-Perez, G. Mao, and Z. Lin, "Performance impact of los and nlos transmissions in dense cellular networks," *IEEE Trans. Wireless Commun.*, vol. 15, no. 3, pp. 2365–2380, Mar. 2016.
- [7] T. Bai and R. W. Heath, "Coverage and rate analysis for millimeter-wave cellular networks," *IEEE Trans. Wireless Commun.*, vol. 14, no. 2, pp. 1100–1114, Feb. 2015.
- [8] M. D. Renzo, "Stochastic geometry modeling and analysis of multi-tier millimeter wave cellular networks," *IEEE Trans. Wireless Commun.*, vol. 14, no. 9, pp. 5038–5057, Sep. 2015.
- [9] S. Singh, M. N. Kulkarni, A. Ghosh, and J. G. Andrews, "Tractable model for rate in self-backhauled millimeter wave cellular networks," *IEEE J. Sel. Areas Commun.*, vol. 33, no. 10, pp. 2196–2211, Oct. 2015.
- [10] Y. Wang and G. d. Veciana, "Dense indoor mmwave wearable networks: Managing interference and scalable mac," in *Proc. 14th WiOpt*, May 2016, pp. 1–8.
- [11] M. I. Kamel, W. Hamouda, and A. M. Youssef, "Multiple association in ultra-dense networks," in *Proc. IEEE ICC*, May 2016, pp. 1–6.
- [12] J. G. Andrews, F. Baccelli, and R. K. Ganti, "A tractable approach to coverage and rate in cellular networks," *IEEE Trans. Commun.*, vol. 59, no. 11, pp. 3122–3134, Nov. 2011.
- [13] B. Blaszczyszyn, M. K. Karray, and H. P. Keeler, "Using poisson processes to model lattice cellular networks," in *Proc. IEEE INFOCOM*, Apr. 2013, pp. 773–781.
- [14] X. Zhang and J. G. Andrews, "Downlink cellular network analysis with multi-slope path loss models," *IEEE Trans. Commun.*, vol. 63, no. 5, pp. 1881–1894, May 2015.
- [15] J. Arnau, I. Atzeni, and M. Kountouris, "Impact of los/nlos propagation and path loss in ultra-dense cellular networks," in *Proc. IEEE ICC*, May 2016, pp. 1–6.
- [16] N. Blaunstein and M. Levin, "Parametric model of uhf/l-wave propagation in city with randomly distributed buildings," in *Proc. IEEE Antennas and Propagation Society International Symposium*, vol. 3, Jun. 1998, pp. 1684–1687.
- [17] T. Bai, R. Vaze, and R. W. Heath, "Analysis of blockage effects on urban cellular networks," *IEEE Trans. Wireless Commun.*, vol. 13, no. 9, pp. 5070–5083, Sep. 2014.
- [18] 3GPP, "Tr 36.828 (v11.0.0): Further enhancements to lte time division duplex (tdd) for downlink-uplink (dl-ul) interference management and traffic adaptation," Jun. 2012.
- [19] G. Mao, B. D. O. Anderson, and B. Fidan, "Online calibration of path loss exponent in wireless sensor networks," in *Proc. IEEE Globecom 2006*, pp. 1–6.
- [20] G. Mao and B. D. O. Anderson, "Graph theoretic models and tools for the analysis of dynamic wireless multihop networks," in *Proc. IEEE WCNC 2009*, pp. 1–6.
- [21] R. Mao and G. Mao, "Road traffic density estimation in vehicular networks," in *Proc. IEEE WCNC 2013*, pp. 4653–4658.
- [22] A. A. Kannan, B. Fidan, and G. Mao, "Robust distributed sensor network localization based on analysis of flip ambiguities," in *Proc. IEEE Globecom 2008*, pp. 1–6.

- [23] S. N. Chiu, D. Stoyan, W. S. Kendall, and J. Mecke, *Stochastic geometry and its applications*. John Wiley & Sons, 2013.
- [24] F. Baccelli and B. Blaszczyzyn, *Stochastic geometry and wireless networks*. Now Publishers Inc, 2009.
- [25] M. Ding, D. Lopez-Perez, G. Mao, P. Wang, and Z. Lin, “Will the area spectral efficiency monotonically grow as small cells go dense?” in *Proc. IEEE GLOBECOM*, Dec. 2015, pp. 1–7.